Published in final edited form as:
Chem Res Toxicol. 2012 January 13; 25(1): 153–161. doi:10.1021/tx200369s.

Altering Iron Oxide Nanoparticle Surface Properties Induce Cortical Neuron Cytotoxicity

Christopher J. Rivet[†,§], **Yuan Yuan**[‡,§], **Diana-Andra Borca-Tasciuc**[‡], and **Ryan J. Gilbert**[†,*]

[†]Center for Biotechnology and Interdisciplinary Studies, Department of Biomedical Engineering, Rensselaer Polytechnic Institute, Troy, NY. 12180-3590

[‡]Department of Mechanical, Aerospace & Nuclear Engineering, Rensselaer Polytechnic Institute, Troy, NY, 12180-3590

Abstract

Superparamagnetic iron oxide nanoparticles, with diameters in the range of a few tens of nanometers, display the ability to cross the blood-brain barrier and are envisioned as diagnostic and therapeutic tools in neuro-medicine. However, despite the numerous applications being explored, insufficient information is available on their potential toxic effect on neurons. While iron oxide has been shown to pose a decreased risk of toxicity, surface functionalization, often employed for targeted delivery, can significantly alter the biological response. This aspect is addressed in the present study, which investigates the response of primary cortical neurons to iron oxide nanoparticles with coatings frequently used in biomedical applications: aminosilane, dextran, and polydimethylamine. Prior to administering the particles to neuronal cultures, each particle type was thoroughly characterized to assess the (1) size of individual nanoparticles, (2) concentration of the particles in solution and (3) agglomeration size and morphology. Culture results show that polydimethylamine functionalized nanoparticles induce cell death at all concentrations tested by swift and complete removal of the plasma membrane. Aminosilane coated particles affected metabolic activity only at higher concentrations while leaving the membrane intact and dextran-coated nanoparticles partially altered viability at higher concentrations. These findings suggest that nanoparticle characterization and primary cell-based cytotoxicity evaluation should be completed prior to applying nanomaterials to the nervous system.

Introduction

Superparamagnetic iron oxide nanoparticles (SPION) are widely used in the biomedical field and have multiple mature and emerging applications such as magnetic resonance imaging (MRI) contrast agents, cell separation media, drug delivery carriers, and cancer hyperthermia.[1,2] Apart from these, SPION are intensively explored in neuro-medicine because they can cross the blood-brain barrier (BBB).[3] Examples of recent developments include the synthesis of enhanced contrast agents for early detection of brain tumors via

*Address correspondence to gilber2@rpi.edu.
§Christopher Rivet and Yuan Yuan contributed equally to this work.

MRI[4–6] as well as magnetic[7] and convection-enhanced[8] drug-delivery systems targeting brain tumor or tissue. In all these applications, the particles are functionalized with different surface chemistries to target specific sites or organelles, enhance cellular uptake or improve retention without deleterious cell reactions.[9–12]

While plain iron oxide nanoparticles pose a low health hazard,[13] surface functionalization can trigger very different cellular responses.[14] For example, Berry *et al.*[15] showed that functionalized iron oxide particles induce alterations in fibroblast cell behavior and morphology distinct from the plain particles. Yet, despite of the multitude of established and emerging neuro-applications for SPION, the cytotoxic potential of these nanomaterials is understated.[16] Moreover, little is known of their interaction with primary neuron cultures, especially when surface functionalization is present. The few studies available in literature examined the response of the PC12 cell line, which are immortalized cells from a pheochromocytoma as well as the C17.2 neural progenitor line.[17, 18] For instance, Pisanic *et al.*[19] showed that exposure to increasing concentrations of anionic magnetic nanoparticles with a dimercaptosuccinic acid coating resulted in a dose-dependent reduction of viability and the capacity of PC12 cells to extend neurites in response to nerve growth factor. Conversely, Kim *et al.*[20] demonstrated that PC12 cells exposed to both polyethylene glycol coated iron oxide nanoparticles and nerve growth factor synergistically increased the efficiency of neurite outgrowth in a dose-dependent manner.

However, to the best of our knowledge, the response of clinically relevant, primary neuronal cells to SPION is yet to be determined. To this end, the present study investigates cytotoxicity using viability and metabolic activity of primary cortical neurons in the presence of iron oxide nanoparticles with three distinct surface coatings frequently used in biomedical applications: aminosilane, dextran, and polydimethylamine. In an attempt to corroborate the mechanism by which nanoparticles affect neuron processes and induce cell death, the underlying material properties were thoroughly characterized using x-ray diffraction (particle size), transmission electron microscopy (particle morphology), vibrating sample magnetometry (particle concentration), and dynamic light scattering (agglomeration size). Nanoparticles are widely available commercially, however manufacturer-provided information is often insufficient or incomplete and proper material characterization of SPION prior to toxicological evaluation is essential. A response by Warheit[21] to an article by Murdock *et al.*[22] emphasizes the importance of critically and accurately defining the nanomaterial properties prior to application to cell cultures. In this paper, the combination of material characterization technologies together with the use of standardized procedures for evaluating cytotoxicity presents a fully developed method for evaluating the influence of SPION on primary neuronal cell cultures.

Experimental Procedures

Particle Size and Morphology

FluidMAG-Amine (aminosilane, Amine), FluidMAG-D (dextran, D) and FluidMAG-PEA (poly-(dimethylamine-co-epichlorhydrin-co-ethylendiamine), PEA) iron oxide nanoparticles were purchased from Chemicell (Berlin, Germany), Figure 1. In all samples the magnetic core is magnetite and the liquid carrier is water. X-ray diffraction (XRD) was utilized to

verify the oxide type and determine the magnetic core size (X'Pert PRO, PANalytical, Westborough, MA). The XRD samples were prepared by air-drying droplets of the stock suspension on a sample holder. The particle size was also assessed using a JEOL 2011 transmission electron microscope (TEM) (Peabody, MA) operating at 200kV. TEM samples were prepared by diluting the stock suspension obtained from the manufacturer with water (1:100), placing a single drop on a carbon-coated copper grid and then air-drying.

Particle Concentration

The magnetization of stock suspensions was measured by a vibrating sample magnetometer (VSM) (Lake Shore Inc., Westerville, OH) to estimate the concentration of the magnetic phase. The measurement was performed at room temperature using approximately 60 μL of stock suspensions. During VSM measurement, sample magnetization was recorded as the function of the applied magnetic field. Field strength was varied in the range of ±1500 kA/m to capture magnetization saturation.

Particle Agglomeration

Dynamic light scattering (DLS) assessment of nanoparticle agglomeration in water and cell culture media was performed using a DynaPro Titan (Wyatt Technology Co., Santa Barbara, CA). Agglomeration of nanoparticle stock suspensions in water was determined by diluting 1:1400 (v/v) with water to provide satisfactory measurement signals. NeuroBasal (NB) media agglomeration was determined by first dispersing the stock solution in NB media at 10% (v/v), replicating the in vitro culture conditions. After incubation to allow for formation of agglomerates, the suspension was further diluted in water to allow for satisfactory measurement of signal production at 1:1400 (v/v).

Zeta Potential

Zeta potential measurements were performed using a Zetaplus analyzer (Brookhaven Instruments Corp., Holtsville, NY) to evaluate the surface charge of the nanoparticles. Zeta potential samples were prepared by diluting nanoparticle samples with deionized (DI) water and NB to 1 mg/mL. The pH value of all samples was 6.7 and the operating temperature was kept constant at 25°C.

Cortical Neuron Isolation and Culture

Cortical neurons were isolated from embryonic day seven chick forebrains in accordance with IACUC approved procedures at Rensselaer Polytechnic Institute. Culture techniques were done in a manner similar to that reported by Sensenbrenner *et al.*[23] Briefly, both lobes of the forebrain were removed, minced and dissociated using 0.25% trypsin. After incubation for 15 minutes, the tissue was dissociated with a micropipette, and Dulbecco's Modified Eagle's Medium (DMEM) supplemented with 10% (v/v) fetal bovine serum (FBS) then inhibited the trypsin. The cell suspension was centrifuged at 500g for 5 minutes to form a cell pellet and the supernatant was then aspirated off. The cells were re-suspended in 1 mL DMEM with 10% (v/v) FBS for counting. Cell density was calculated and the suspension was distributed to a 24 well plate at a density of 500,000 cells per well. All wells were pre-coated with 0.01% (w/v) poly-L-lysine for 2 hours at 37°C. Two hours after initial plating,

the media was exchanged with NB medium containing 2% (v/v) B-27 supplement, 1% (v/v) penicillin/streptomycin, and 0.5 mM L-glutamine.

Neuronal verification was performed by immunohistochemistry staining using RT97 neurofilament primary antibody (Developmental Studies Hybridoma Bank, Iowa City, IA) with a donkey anti-mouse Alexa 594 secondary antibody. Nuclei were stained using 4',6-diamidino-2-phenylindole (DAPI). Briefly, neurons were fixed in 4% paraformaldehyde at 4°C for one hour, washed twice with phosphate buffered saline (PBS) (1×, pH 7.4) and blocked for one hour in 5% bovine serum albumin (BSA) in PBS containing 0.4% (v/v) Triton X-100 at room temperature. The primary antibody was then diluted in an incubation solution containing 0.5% BSA and 0.1% (v/v) Tween-20 in PBS at 1:500 and incubated overnight at 4°C. This solution was then removed and the cells were washed three times in 0.1% (v/v) Tween-20 in PBS. The cells were washed three times and incubated with the secondary antibody diluted 1:1000 in incubation solution containing DAPI (1 μg/mL) for one hour. Samples were then washed twice in PBS and imaged.

Viability Analysis

Cortical neuron viability was assessed using calcein-AM, a molecule that becomes fluorescent upon esterase degradation by viable cells. Neurons were incubated for 48 hours after initial plating to allow for attachment and neurite elongation. The NB media was removed and replaced with NB containing 1, 5, or 10% (v/v) of each nanoparticle solution (10, 50 or 100 μL of stock particle solution per mL culture media). After 24 hours of incubation in the presence of nanoparticles, half of the media (250 μL) was removed, replaced with 250 μL of propidium iodide solution (2 μg/mL in PBS) and incubated for 30 minutes. Half of the media (250 μL) was once again removed, replaced with 250 μL of calcein-AM solution (2 μg/mL in PBS) and incubated for 15 minutes. The media was then completely removed and washed once with PBS and imaged using a 20× objective. Three images per well were captured with constant exposure and gain settings using an Olympus DSU (Center Valley, PA). The response of cortical neurons to SPION was done in duplicate for each combination of nanoparticle type and concentration, and the entire procedure was performed twice (n = 12 per condition). For quantitative analysis, each calcein-AM image was then first converted to a binary format and subsequently measured for percent area covered by the fluorescent neurons using ImageJ (National Institutes of Health, Bethesda, MD).

Metabolic Assay

Similar to the viability analysis above, neurons were incubated for 48 hours after initial plating before nanoparticle addition. The media was removed and replaced with NB containing 1, 5, or 10% (v/v) of nanoparticle solution. There were two samples created for each particle condition, one to be used as the experimental sample and one to serve as a corresponding control. After 24 hours of incubation, 100 μL of 3-(4,5-dimethylthiazol-2-yl)-5-(3-carboxymethoxyphenyl)-2-(4-sulfophenyl)-2H-tetrazolium (MTS) (Promega, Madison, WI) solution was added to each experimental sample and 100 μL of NB media was added to the corresponding control samples. The well plate was incubated for four hours, and duplicate 200 μL samples of the media were collected for analysis. Each sample

was then diluted 4× to reduce sample density and measured for absorbance of light in a 96 well plate at 490nm in a multiwell plate reader (Perkin Elmer Envision 2104, Waltham, MA). The entire procedure was performed twice (n = 4 per condition). The background absorbance created by the corresponding control (containing nanoparticles, without MTS solution) was subtracted from the experimental sample. Each corrected particle sample was then normalized to a control sample (without nanoparticles) that was also corrected for background absorbance.

Scanning Electron Microscopy

Cortical neurons were cultured in 4-well chamber slides at a density of 250,000 cells per well for qualitative analysis by scanning electron microscopy (SEM). Neurons were exposed to nanoparticles as described in the previous sections and fixed for one hour using a 4% (w/v) paraformaldehyde solution in PBS. Samples were then stained with a 2% (w/v) osmium tetroxide (Sigma Aldrich, St. Louis, MO) solution for one hour and serially dehydrated in ethanol (70, 80, 90 and 100% (v/v) for 5 minutes each). The sample was then prepared for SEM by first critical point drying and subsequently coating with a 5 nm layer of platinum. SEM samples were imaged using a Zeiss Supra55 (Peabody, MA) at 3kV.

Membrane Disruption

Cortical neurons were seeded at a density of 500,000 cells per well in a 0.01% (w/v) poly-L-lysine pre-coated 24 well plate similar to above. After 48 hours of attachment, the media was removed and replaced with a 1:1 mixture of NB and 4 μg/mL calcein-AM in PBS. The cells were incubated for 15 minutes and the media was aspirated off. The cells were then washed once with fresh NB media after which NB media containing 5% (v/v) PEA particles was added to the culture. Images were captured at 1, 2, 3, 4, and 8 hours. All samples were compared to control groups (no particles). Each sample was done in duplicate.

Statistical Analysis

Results from the metabolic assay and viability image analysis were statistically evaluated using a one-way ANOVA through the use of JMP software (SAS, Cary, NC). A Tukey-HSD post-hoc test was used to compare all pairs of means. A p-value less than 0.05 were considered statistically significant.

Results

Nanoparticle Characterization

First, X-ray diffraction (XRD) was used to determine the magnetite (iron oxide) core size by generating spectra of three particle samples. The XRD spectra of all three samples (Figure 2A) match the standard magnetite (Fe_3O_4) crystal structure data.[24] In this study the superparamagnetic properties of the magnetite core are not being employed, however; it is still important to quantify that this parameter is consistent among the different particles used. The observed peak broadening effect is due to the small particle size. The maximum peak width at half height among the six most significant peaks was utilized to calculate the crystal size[25] from:

$$d_{CRYS}=\frac{0.93\lambda}{B_{1/2}\cos\theta}$$

Where d^{CRYS} is the crystallite size (nm), λ is the used X-ray wavelength (1.54 Å), $B_{1/2}$ is the maximum peak width at half height, and θ is the Bragg's angle (degrees). From the XRD measurements, the average diameter of the magnetite core for Amine, D and PEA coated particles was calculated to be 9.4 nm, 9.0 nm and 8.1 nm respectively.

The room temperature magnetization curves (Figure 2B) generated by a vibrating sample magnetometer (VSM) permit calculation of mass concentration for each particle type. The absence of a hysteresis loop indicates that the particles in all three solutions are superparamagnetic, consisting of magnetic monodomains, which is expected for this range of particle size. In principle, the volume fraction of the magnetite phase (ϕ) can be determined from:

$$\varphi=\frac{M_S}{M_B}$$

where M_S is the saturation magnetization of the magnetic fluid (taken from magnetization curves) and M_B is the saturation magnetization of bulk iron oxide (4.46 × 10^5 A/m).[26] However, for coated nanoparticles, the magnetic core can interact with the functional layer to form a nonmagnetic compound, and M_S decreases below $M_B\phi$.[27] For instance, in water-based ferrofluids with particle sizes around 10 nm, the measured M_s has been reported as 76% of the product between volume concentration of the magnetic phase and its saturation magnetization in bulk.[28] Therefore, the real volume fraction of nanoparticles (ϕ_M) can be up to 30% higher than ϕ, an effect taken into consideration here. Once the volumetric concentration is determined, the mass concentration is calculated from:

$$\rho_M=\rho\times\varphi_M$$

where ρ is the mass density of magnetite (5.18 g/mL).[27] The calculated mass concentrations of Amine, PEA and D particles are 39.3 mg/mL, 60.5 mg/mL and 53.1 mg/mL respectively. These values are significantly higher than that supplied by the manufacturer, which listed all particle solutions at 25 mg/mL.

Transmitted electron microscopy (TEM) images of Amine, D and PEA particles (Figures 3A–C) verify that the magnetite core diameter was approximately 10 nm. In addition, these images suggested the presence of agglomeration in all three suspensions. To verify this, dynamic light scattering (DLS) studies were performed. Initially, these measurements were recorded on water-diluted samples. However, agglomeration may change with the dispersion medium,[29] and therefore measurements in culture media were also acquired. Prior to DLS measurement, nanoparticles were added to NeuroBasal (NB) culture media at a concentration of 10% (v/v) and the solutions were vortexed to ensure full dispersion. Noticeable sedimentation occurred for Amine and PEA particles (Figures 4A & C) after one

hour but the D particles (Figure 4B) were stably suspended in the NB media. The DLS analysis graph (Figure 4D) shows that the average agglomerate sizes of Amine, D and PEA particles diluted in water are found to be 45.3 nm, 24.7 nm and 47.5 nm respectively. Their average agglomerate sizes change to 56.4 nm, 20.6 nm and 8.6 nm when NB media is the dilution medium. Therefore, it is concluded that dilution medium affects agglomerate sizes of Amine and especially PEA groups, whereas culture media did not affect the agglomerate size of D coated particles.

Zeta potential analysis of the SPION shows a strong correlation between hydrodynamic radiuses, as determined by the DLS measurements, with the zeta potential of the particles in DI water, Figure 4E. This correlation is then lost for the Amine group when comparing the particle types dispersed within NB medium, as this group exhibits a significant change within the zeta potential analysis but not in the DLS measurements. The D particles exhibit a similar response to alterations in dispersion medium through both techniques, where they appear to be unaffected by these changes, likely due to their chemical composition. The PEA particles also follow a similar trend between measurements, indicating that protein interactions in the dispersion medium induce significant alterations agglomeration and surface charge.

Cortical neuron toxicity

Dissociated cortical neurons isolated from embryonic day 7 chicks were assessed for culture purity by determining the co-localization of RT97 neurofilament antibody and with the nuclear stain DAPI (Figure 5A). Greater than 95% of the cells in culture were neurons (data not shown), since most of the nuclei were present in cells staining positive for RT97, which is found exclusively in neurons. Very few, if any, viable, DAPI-stained nuclei were found in areas not also expressing neurofilament.

The effect of SPION on neuron viability was evaluated through the fluorescent indicator of cellular viability (calcein-AM) via intracellular enzymatic activity and for membrane disruption (propidium iodide). Neurons were cultured for 48 hours to allow for attachment and extension of neurites prior to addition of SPION containing media. The media contained particles in three different concentrations (1, 5, and 10% (v/v) of stock particle solution in NB media) for each of the three coating types (Amine, D, PEA) creating nine total combinations (Amine1, Amine5, Amine10, etc.) plus a control (no particles). After 24 hours of culture, viable cells were visualized by the enzymatic degradation of calcein-AM, fluorescently labeling the entire neuron green and the nuclei of dead cells were stained red by propidium iodide. The high concentration (10% v/v) Amine and D groups (Figures 5C & D) appeared morphologically similar to that of the control (Figure 5B) where neurite processes are present and extensive. Similarly, the number of dead cells in these images appears equal, with slightly more in the D group. The high concentration group of the PEA particles (Figure 5E) significantly reduced the number of viable neurons present and those that did remain viable were in a compromised state, as distinguished by their bulbous appearance. There was also a significant increase in dead cells in this group as compared to the other groups.

Correlating viability and metabolic rate

Quantification of the images was performed to determine if statistically significant, SPION-dependent effects occurred. All images were first converted to a binary format using a constant threshold value and subsequently measured for percent area covered by fluorescent neurons. The percent area covered per image by viable cells for each condition was averaged and normalized relative to the control (Figure 6A). The Amine particles did not significantly reduce viability as compared to the control, although a slight decrease in viability was observed with the higher concentration groups. The lowest concentration of D particles did not induce a statistically significant reduction in viability, but the higher concentrations did. The PEA particles induced a significant reduction in viability. The lowest PEA particle concentration produced a viability measurement that was 12% of the control and the higher PEA particle concentrations produced a viability measurement that was approximately 5% of the control after 24 hours of particle incubation.

These results were then further reinforced through the use of an MTS metabolic assay (Figure 6B). Once again, the PEA group displayed a statistically significant reduction in metabolic activity as compared to the other groups. However, using this assay, the Amine particles exhibited a concentration-dependent response, where the 5 and 10% samples were significantly reduced as compared to the control. The concentration-dependent response as exhibited by the 5 and 10% D samples in the viability assay was lost after analyzing cell metabolism effects, indicating that nanoparticle induced changes in cell metabolism with certain particles may not correlate directly with changes in viability.

Morphological response to SPION

Since the PEA particles were the most cytotoxic, the mechanism by which the cytotoxicity occurred was investigated. It was observed that the neurons in the PEA groups were still attached to the culture substrate after the cytotoxic effect had run its course, as their nuclei were visible in images using propidium iodide. Thus, the cells must undergo apoptosis/necrosis at a rate that would leave the cells attached to the substrate and not permit retraction/removal. Therefore, the neurons were fixed with paraformaldehyde and prepared for scanning electron microscopy (SEM) imaging to investigate the physical interaction between the cells and the SPIONs. The control, Amine and D (Figures 7A–C) all appeared as anticipated with slight morphological changes occurring the Amine group, likely due to the effects of particle sedimentation. However, in the PEA group (Figure 7D) the plasma membrane of the neurons is completely removed, exposing the cytoskeletal network below. Closer examination of the cell (Figure 7E) clearly displays the extent of removal. This effect was observed at both the 5 and 10% (v/v) concentrations of the PEA samples.

Imaging membrane disruption

In attempt to support the mechanism of membrane removal, the integrity of the plasma membrane was monitored over time as PEA particles were administered to the culture (Figure 8). The cytoplasm was loaded with calcein-AM prior to addition of particles and when the membrane was compromised, the fluorescent molecule was released and the intensity of the cellular signal becomes reduced. The control sample (Figure 8A) remained bright after one hour whereas the PEA group (Figure 8B) was significantly reduced. At this

time point it appears that some, but not all of the cells are affected by the particles. However, at eight hours after administering the particles (Figure 8C), cellular brightness is uniformly reduced and the control remained unchanged (not shown). Upon closer inspection (Figure 8D), the nuclei are clearly visible as bright dots within the cells, indicating that the membrane is no longer present.

Discussion

The goal of this study was to investigate the cytotoxic effect of SPION with three distinct coatings when administered to primary cortical neuron cultures at three concentrations. The particles were purchased from a commercial manufacturer and are listed for biological applications. The aminosilane (Amine) and poly-(dimethylamine-co-epichlorhydrin-co-ethylendiamine) (PEA) particles (Figures 1A & C) contain a terminal amine group, which is beneficial for use with EDC/NHS conjugation systems to add targeting ligands or therapeutics. Particles with the dextran (D) coating (Figure 1B) are routinely used for MRI applications.[30] Therefore, it was hypothesized that these three unique coatings would be of interest for cytotoxic evaluation due to their relevance in biomedical applications.

Publications employing the use of neuronal or glial primary cells with iron oxide nanoparticles are scarce; however one reports the use of rat astrocytes.[31] Astrocytes, neurons, oligodendrocytes and microglia are the predominant cell populations within the central nervous system, thus; assessing their cytotoxic response to SPION, which may cross the BBB and accumulate within the brain (*3*), is essential. The potentially cytotoxic effects of SPION on central nervous system cells *in vivo* may arise from one of two pathways: (1) the particles are administered systemically and accumulate within the brain or (2) the particles are directly injected into the brain. The latter is a more likely mode given current applications; however, BBB permeability is increased in tumors, presenting a potentially viable access point for systemic administration of nanoparticles.[32] Therefore, in attempt to better understand the interaction between SPION and the different cells and tissues to which they are subjected, the particles themselves must be first rigorously characterized to reduce the variables present.

Defining the size, morphology, concentration and agglomeration provides the necessary information to properly define the SPION being investigated. Each one of these parameters is reported to influence the cytotoxic response. Mahmoudi *et al.*[33] reported that both particle shape and particle size influence toxicity while Karlsson *et al.*[34] found that particle composition and size may also influence toxicity. Furthermore, Ge *et al.*[35] found agglomeration and surface charge dependent effects on particle uptake and subsequent toxicity while Naqvi *et al.*[36] reported concentration dependent toxicity. It is interesting to note that the concentration of the particles as listed by the manufacturer (25 mg/mL) was significantly lower than that quantified through the use of VSM (~50 mg/mL), further reinforcing the need for thorough characterization prior to cytotoxicity evaluation. Therefore, XRD, VSM, TEM and DLS were used to quantify the necessary parameters and display that all particle types were morphologically and physically similar and that the only difference between the particle types is their agglomeration and sedimentation potential, which is directly related to the surface chemistries of the Amine and PEA particles.

Primary cortical neurons were chosen as an indicator of cytotoxicity based on (1) immortalized cell lines, such as PC12 cells, may be more resilient to particle-induced toxicity due to their oncogenic modification and (2) SPION are of a size where they may pass the BBB and directly interact with neurons *in vivo*. However, the most frequent concern with using primary cells is the lack of culture homogeneity. Our model was found to be highly reproducible with only a small percentage of non-neuronal cells present due to the developmental stage from which the cells are isolated, eliminating non-neuronal progenitors.[23]

Based on the results presented herein, the Amine and D particles are worthy candidates for future investigations while the PEA particles are most certainly not as they were proven to induce toxic effects. These results were illustrated through multiple mediums: qualitative cell morphology, quantitative image analysis and metabolic activity. All three methods arrive at the same conclusion for the PEA particles, whereas the Amine particles display a significant concentration-dependent decrease only in metabolic activity, and not in viability as anticipated. This inconsistency is likely due to the fact that the cells undergo changes when Amine particle sedimentation occurs, as this forms a dense cover over the cells, limiting nutrient exchange. This phenomenon is also exhibited within the high PEA concentration group in (Figure 5E) where the few remaining viable cells become more sphere-like, indicating that the dense coating can influence morphology as well.

Rupture of the cellular membrane is potentially due to the chemical structure of the PEA coating, where the positively-charged terminal amine may initially facilitate interaction with cell's negatively charged glycocalyx. Once in close proximity, the internal hydrophobic domains within PEA may permit rapid internalization of the particles into the cytoplasm or the external removal of the plasma membrane phospholipids. Singular nanoparticles may enter a cell, whereas it may be more difficult for large agglomerates. Presence of these isolated particles is supported by the DLS analysis (Figure 4D), where particles were found to be on average 10 nm in radius. However, SEM images (Figure 7E) display the creation of significantly larger agglomerates in direct contact with the membrane. These larger agglomerates may be the result of complexes formed between the sequestered phospholipids and the PEA particles. Alternatively, complexes may arise due to interactions with proteins found in the NB medium, potentially coating the particle and permitting a direct interaction with the cellular membrane. Changes in the zeta potential value for the Amine and PEA groups indicate that protein within the NB media may interact with the particles, whereas this does not occur with the dextran coated particles. The reaction to the NB by the Amine particles actually changes the surface charge from positive to negative, which can drastically influence the ability of these particles to interact with the cellular membrane. This supports the metabolic activity decrease and not viability decrease as displayed in Figure 6, as the particles may be hindering nutrient exchange but not manipulating membrane integrity. Thus, the mechanism by which the PEA particles remove the membrane is likely due to external interactions where the chemical structure of this coating sequesters the phospholipid bilayer. This is an important finding as these particles are labeled for biological use, while our studies suggest that have potentially hazardous cellular effects.

The number of applications for iron oxide nanoparticles will increase as the technology matures in terms of finite particle control through external electromagnetic fields or by cell-specific targeting through the use of conjugated ligands or therapeutics. However, the progress of technological forefronts often precedes the necessary precautionary steps to ensure safety to those applying the technology as well as the subjects onto which it is applied. The surface chemistry of the PEA particles undoubtedly induces plasma membrane removal and subsequent neuronal death. While similar results have yet to be determined for other cell types, this is highly probable as plasma membranes are all constructed of phospholipids. This chemistry-specific mechanism is definite because Amine and D particles with similar size and shape produce opposing results when applied at similar concentrations. Thus, quantifying all particle variables in addition to utilizing multiple cytotoxic metrics can be a powerful investigative tool for understanding the effects of emerging nanomaterials.

Acknowledgments

The authors thank Drs. Chris Bjornsson and Cynthia Collins of the Center for Biotechnology and Interdisciplinary studies at Rensselaer Polytechnic Institute for aiding in microscopy and plate reader use respectively. David Frey of the Micro and Nano Fabrication Clean Room for assisting with SEM imaging. The RT97 monoclonal antibody developed by J. Wood was obtained from the Developmental Studies Hybridoma Bank developed under the auspices of the NICHD and maintained by The University of Iowa, Department of Biology, Iowa City, IA 52242.

Funding

Funding was provided by support from the National Institutes of Health, National Institute of Neurological Disorders and Stroke R21NS62392 to R.J.G. D.-A. B.-T. acknowledges support from National Science Foundation through grants 0846433 and 0708521.

Abbreviations

SPION	Superparamagnetic iron oxide nanoparticles
BBB	Blood-brain barrier
Amine	Aminosilane
D	Dextran
PEA	poly-(dimethylamine-co-epichlorhydrin-co-ethylendiamine)
VSM	vibrating sample magnetometer
NB	NeuroBasal
DMEM	Dulbecco’s Modified Eagle’s Medium
FBS	fetal bovine serum
DAPI	4', 6-diamidino-2-phenylindole
MTS	3-(4, 5-dimethylthiazol-2-yl)-5-(3-carboxymethoxyphenyl)-2-(4-sulfophenyl)-2H-tetrazolium

Reference

1. Pankhurst QA, Connolly J, Jones SK, Dobson J. Applications of magnetic nanoparticles in biomedicine. J Phys D: Appl Phys. 2003; 36:R167–R181.
2. Krishnan KM. Biomedical nanomagnetics: a spin through possibilities in imaging, diagnostics, and therapy. IEEE Trans Magn. 2010; 46:2523–2558. [PubMed: 20930943]
3. Wang J, Chen Y, Chen B, Ding J, Xia G, Gao C, Cheng J, Jin N, Zhou Y, Li X, et al. Pharmacokinetic parameters and tissue distribution of magnetic Fe(3)O(4) nanoparticles in mice. Int J Nanomedicine. 2010; 5:861–866. [PubMed: 21042548]
4. Kumar M, Medarova Z, Pantazopoulos P, Dai G, Moore A. Novel membranepermeable contrast agent for brain tumor detection by MRI. Magn Reson Med. 2010; 63:617–624. [PubMed: 20146231]
5. Sun C, Veiseh O, Gunn J, Hansen S, Lee D, Sze R, Ellenbogen RG, Olson J, Zhang M. In vivo MRI detection of gliomas by chlorotoxin-conjugated superparamagnetic nanoprobes. Small. 2008; 4:372–379. [PubMed: 18232053]
6. Yu F, Zhang L, Huang Y, Sun K, David AE, Yang VC. The magnetophoretic mobility and superparamagnetism of core-shell iron oxide nanoparticles with dual targeting and imaging functionality. Biomaterials. 2010; 31:5842–5848. [PubMed: 20434209]
7. Chertok B, David AE, Yang VC. Polyethyleneimine-modified iron oxide nanoparticles for brain tumor drug delivery using magnetic targeting and intra-carotid administration. Biomaterials. 2010; 31:6317–6324. [PubMed: 20494439]
8. Perlstein B, Ram Z, Daniels D, Ocherashvilli A, Roth Y, Margel S, Mardor Y. Convection-enhanced delivery of maghemite nanoparticles: increased efficacy and MRI monitoring. Neuro-oncology. 2008; 10:153–161. [PubMed: 18316474]
9. Gupta AK, Gupta M. Synthesis and surface engineering of iron oxide nanoparticles for biomedical applications. Biomaterials. 2005; 26:3995–4021. [PubMed: 15626447]
10. Cengelli F, Maysinger D, Tschudi-Monnet F, Montet X, Corot C, Petri-Fink A, Hofmann H, Juillerat-Jeanneret L. Interaction of functionalized superparamagnetic iron oxide nanoparticles with brain structures. J Pharmacol Exp Ther. 2006; 318:108–116. [PubMed: 16608917]
11. Berry CC, Well S, Charles S, Aitchison G, Curtis AS. Cell response to dextran-derivatised iron oxide nanoparticles post internalization. Biomaterials. 2004; 25:5405–5413. [PubMed: 15130725]
12. Gupta AK, Curtis AS. Surface modified superparamagnetic nanoparticles for drug delivery: interaction studies with human fibroblasts in culture. J Mater Sci: Mater Med. 2004; 15:493–496. [PubMed: 15332623]
13. Liu S, Han Y, Yin L, Long L, Liu R. Toxicology studies of a superparamagnetic iron oxide nanoparticle in vivo. Advanced Materials Research. 2008; 47–50:1097–1100.
14. Ying E, Hwang HM. In vitro evaluation of the cytotoxicity of iron oxide nanoparticles with different coatings and different sizes in A3 human T lymphocytes. Sci Total Environ. 2010; 408(20):4475–4481. [PubMed: 20673962]
15. Berry CC, Wells S, Charles S, Curtis AS. Dextran and albumin derivatized iron oxide nanoparticles: influence on fibroblasts in vitro. Biomaterials. 2003; 24:4551–4557. [PubMed: 12950997]
16. Kunzmann A, Andersson B, Thurnherr T, Krug H, Scheynius A, Fadeel B. Toxicology of engineered nanomaterials: focus on biocompatibility, biodistribution and biodegradation. Biochim Biophys Acta. 2011; 1810(3):361–373. [PubMed: 20435096]
17. Soenen SJ, Himmelreich U, Nuytten N, Pisanic TR 2nd, Ferrari A, De Cuyper M. Intracellular nanoparticle coating stability determines nanoparticle diagnostics efficacy and cell functionality. Small. 2010 Oct 4; 6(19):2136–2145. [PubMed: 20818621]
18. Soenen SJ, Himmelreich U, Nuytten N, De Cuyper M. Cytotoxic effects of iron oxide nanoparticles and implications for safety in cell labelling. Biomaterials. 2011 Jan; 32(1):195–205. [PubMed: 20863560]
19. Pisanic TR II, Blackwell JD, Shubayev VI, Finones RR, Jin Sungho. Nanotoxicity of iron oxide nanoparticles internalization in growing neurons. Biomaterials. 2007; 28:2572–2581. [PubMed: 17320946]

20. Kim JA, Lee N, Kim BH, Rhee WJ, Yoon S, Hyeon T, Park TH. Enhancement of neurite outgrowth in PC12 cells by iron oxide nanoparticles. Biomaterials. 2011; 32:2871–2877. [PubMed: 21288566]
21. Warheit DB. How meaningful are the results of nanotoxicity studies in the absence of adequate material characterization? Toxicol Sci. 2008; 101(2):183–185. [PubMed: 18300382]
22. Murdock RC, Braydich-Stolle L, Schrand AM, Schlager JJ, Hussain SM. Characterization of nanomaterial dispersion in solution prior to in vitro exposure using dynamic light scattering technique. Toxicol Sci. 2008; 101(2):239–253. [PubMed: 17872897]
23. Sensenbrenner M, Maderspach K, Latzkovits L, Jaros GG. Neuronal cells from chick embryo cerebral hemispheres cultivated on polylysine-coated surfaces. Dev Neurosci. 1978; 1(2):90–101. [PubMed: 755685]
24. Guinier, A. X-ray diffraction in crystals, imperfect crystals, and amorphous bodies. Freeman, San Francisco: 1963. p. 378
25. Rovers SA, van der Poel LAM, Dietz CHJT, Noijen JJ, Hoogenboom R, Kemmere MF, Kopinga K, Keurentjes JTF. Characterization and magnetic heating of commercial superparamagnetic iron oxide naoparticles. J Phys Chem. 2009; 113:14638–14643.
26. Rosensweig RE. Heating magnetic fluid with alternating magnetic field. J Magn Magn Mater. 2002; 252:370–374.
27. Chantrell RW, Popplewell J, Charles SW. Measurements of particle size distribution parameters in ferrofluids. IEEE Trans Magn. 1978; 14(5):975–977.
28. Kaiser R, Miskolczy G. Magnetic properties of stable dispersions of subdomain magnetite particles. J Appl Phys. 1970; 41(3):1064–1072.
29. Hinderliter PM, Minard KR, Orr G, Chrisler WB, Thrall BD, Pounds JG, Teeguarden JG. ISDD: A computational model of particle sedimentation, diffusion and target cell dosimetry for in vitro toxicity studies. Part Fibre Toxicol. 2010; 7(1):36. [PubMed: 21118529]
30. Tassa C, Shaw SY, Weissleder R. Dextran-Coated Iron Oxide Nanoparticles: A Versatile Platform for Targeted Molecular Imaging, Molecular Diagnostics, and Therapy. Acc Chem Res. 2011 In press.
31. Geppert M, Hohnholt MC, Thiel K, Nürnberger S, Grunwald I, Rezwan K, Dringen R. Uptake of dimercaptosuccinate-coated magnetic iron oxide nanoparticles by cultured brain astrocytes. Nanotechnology. 2011; 22(14):145101. [PubMed: 21346306]
32. Hobbs SK, Monsky WL, Yuan F, Roberts WG, Griffith L, Torchilin VP, Jain RK. Regulation of transport pathways in tumor vessels: role of tumor type and microenvironment. Proc Natl Acad Sci U S A. 1998; 95(8):4607–4612. [PubMed: 9539785]
33. Mahmoudi M, Simchi A, Milani AS, Stroeve P. Cell toxicity of superparamagnetic iron oxide nanoparticles. J Colloid Interface Sci. 2009; 336(2):510–518. [PubMed: 19476952]
34. Karlsson HL, Gustafsson J, Cronholm P, Möller L. Size-dependent toxicity of metal oxide particles--a comparison between nano- and micrometer size. Toxicol Lett. 2009; 188(2):112–118. [PubMed: 19446243]
35. Ge Y, Zhang Y, Xia J, Ma M, He S, Nie F, Gu N. Effect of surface charge and agglomerate degree of magnetic iron oxide nanoparticles on KB cellular uptake in vitro. Colloids Surf B Biointerfaces. 2009; 73(2):294–301. [PubMed: 19564099]
36. Naqvi S, Samim M, Abdin M, Ahmed FJ, Maitra A, Prashant C, Dinda AK. Concentration-dependent toxicity of iron oxide nanoparticles mediated by increased oxidative stress. Int J Nanomedicine. 2010; 5:983–989. [PubMed: 21187917]

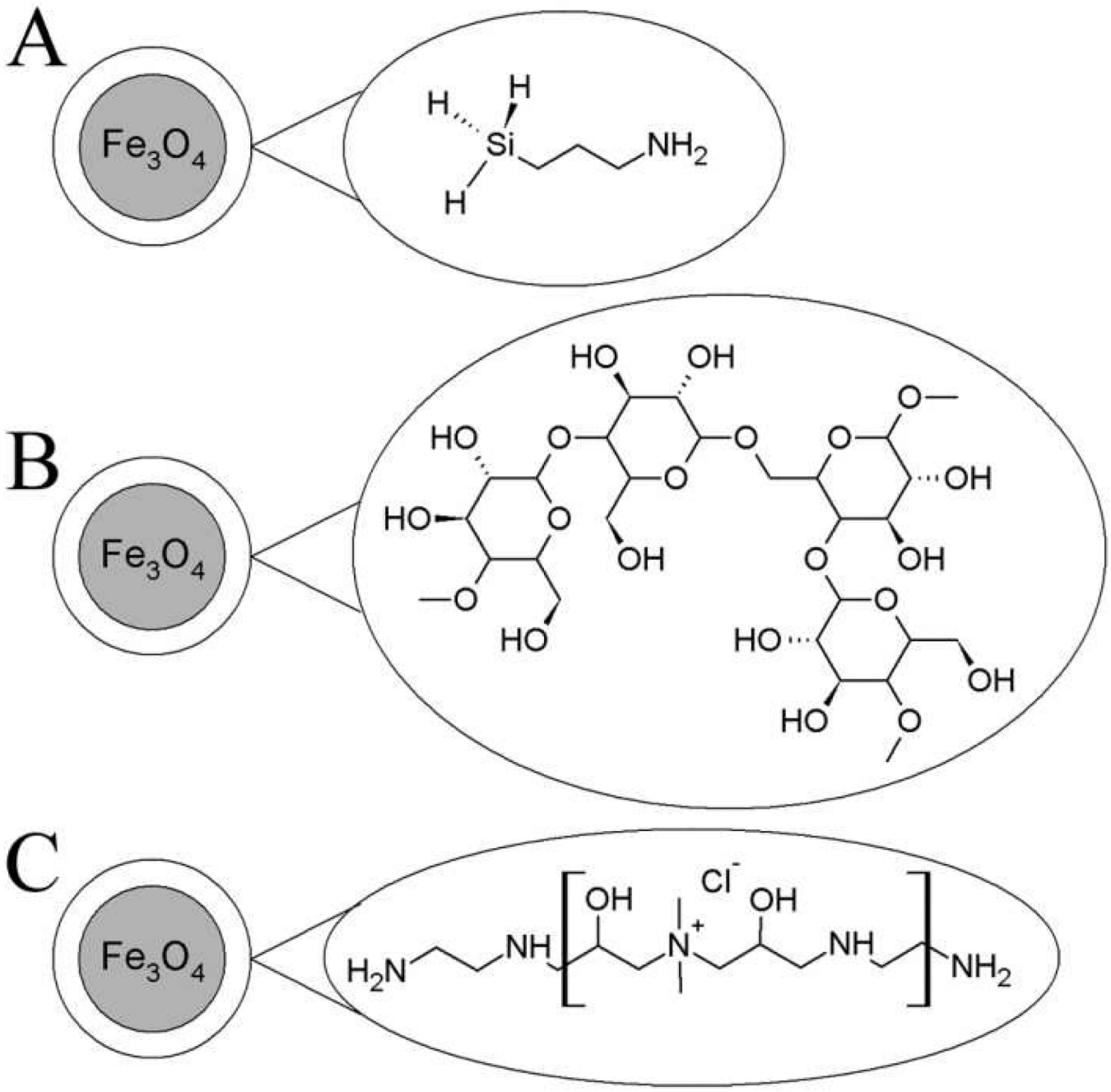

Figure 1.

Chemical structures of functionalized iron oxide nanoparticles. Samples were purchased with (A) aminosilane (Amine), (B) dextran (D) and (C) poly-(dimethylamine-co-epichlorhydrin-co-ethylendiamine) (PEA) coatings.

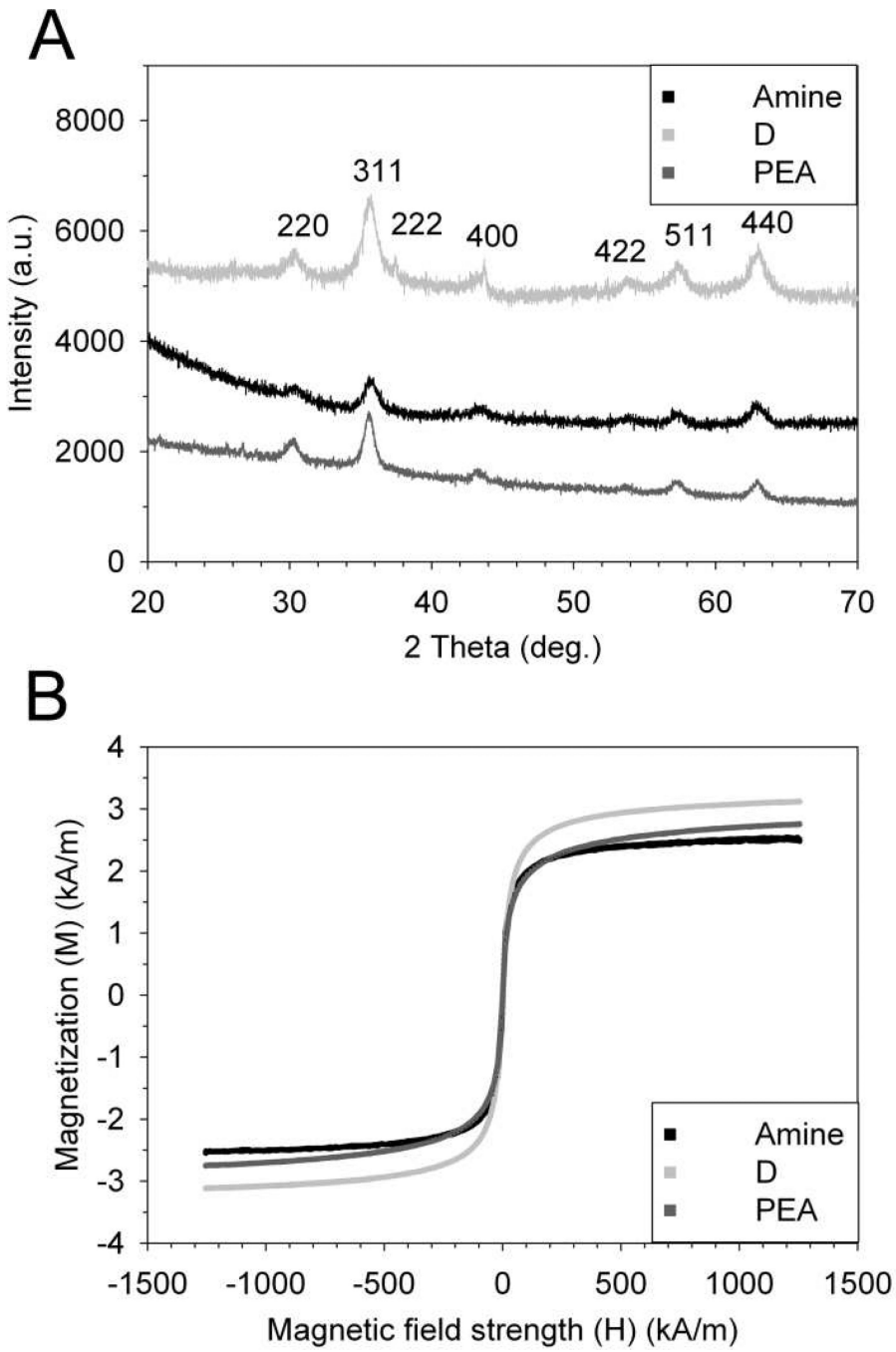

Figure 2.

Characterization of the iron oxide core encapsulated within the various surface coatings. (A) X-ray diffraction patterns of iron oxide nanoparticle suspensions. All corresponding peaks are matched to the standard pattern of magnetite. (B) Magnetization curves of iron oxide nanoparticle suspensions. The absence of a hysteresis loop indicates that the nanoparticles possess superparamagnetic properties. The saturation magnetizations are utilized to calculate volume concentration of iron oxide nanoparticles.

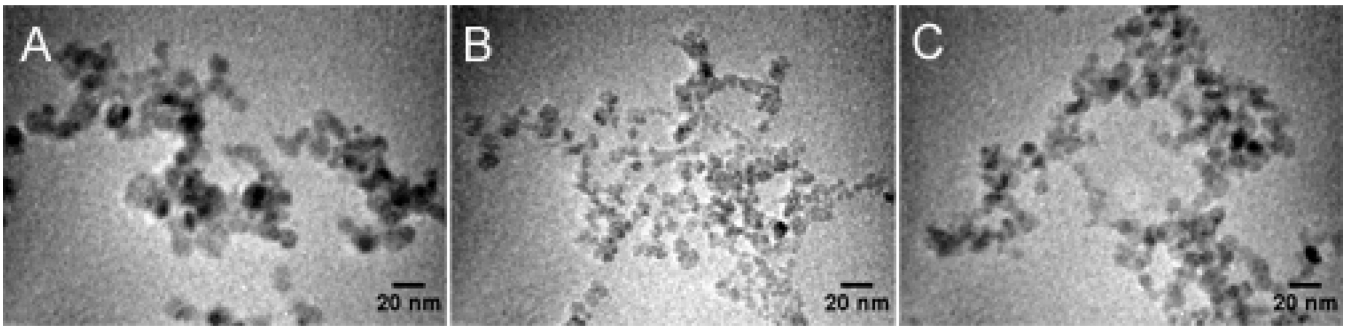

Figure 3.

Transmission electron microscopy (TEM) images of iron oxide nanoparticles with various surface coatings. Nanoparticles with (A) Amine, (B) D and (C) PEA surface chemistries all display agglomeration when diluted in water. The dark regions represent the magnetite (iron oxide) core while the lighter regions are the coating shell.

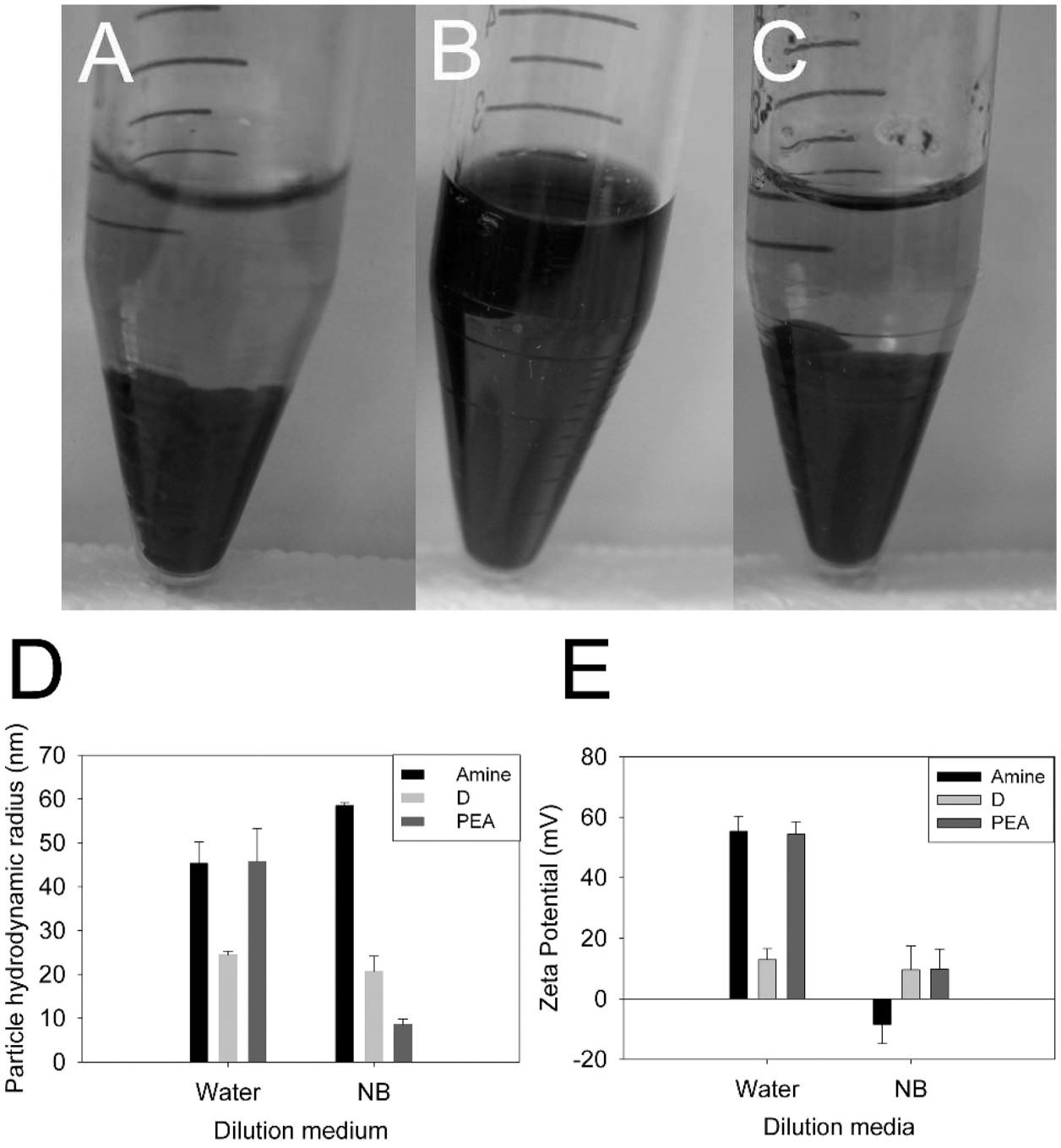

Figure 4.

Sedimentation effects and quantification of agglomerate size of SPION with various surface coatings. Visual inspection of sedimentation one hour after mixing when nanoparticles with (A) Amine, (B) D and (C) PEA surface chemistries are diluted to 10% (v/v) in NeuroBasal (NB) media. (D) Quantification of agglomerate sizes of iron oxide nanoparticles dispersed in water and NB media. Dispersion medium significantly alters the agglomerate size of PEA coated samples while Amine and D coated particles are minimally influenced. The surface charge of the particles was also measured through zeta potential analysis (E). The DLS

results express a correlation to the zeta potential measurements with water as a dispersion medium, this effect is then lost when NB media is used, likely due to protein interactions with the polymeric coatings.

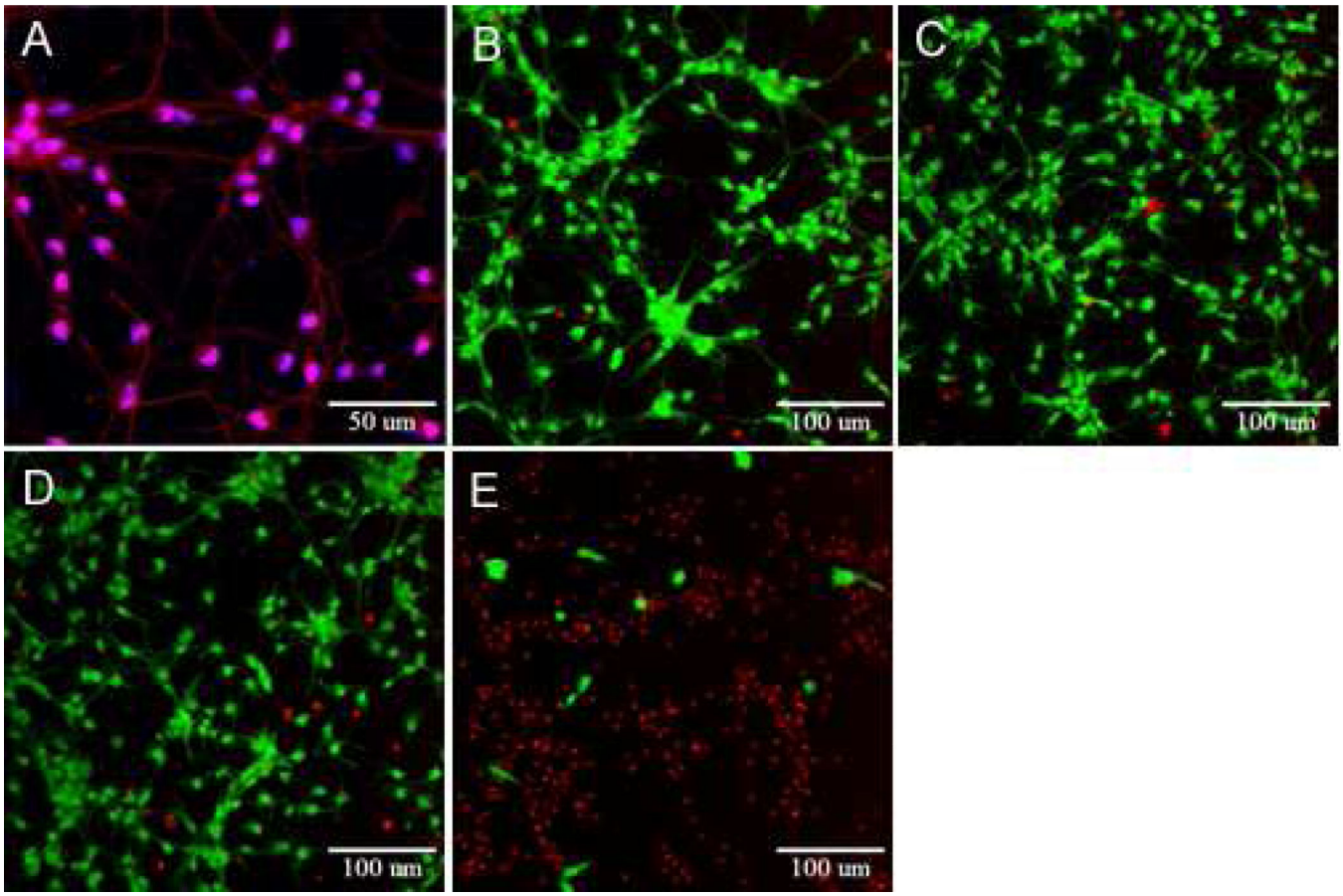

Figure 5.

Cytotoxic effects of iron oxide nanoparticles with varying surface chemistry on cortical neurons. Cortical neuron verification was performed by (A) staining with RT97 neurofilament antibody (red) and DAPI for nuclei (blue). Overlapping RT97 and DAPI signals indicate neurons. Viability was assessed through the enzymatic degradation of calcein-AM (green) and permeability to propidium iodide (red) after 24 hours exposure to (B) control (C) Amine (D) D and (E) PEA particles all at 10% (v/v) in NB media. The PEA group exhibited a significant reduction in cell number as well as morphological changes while all other groups remained unchanged. All images were captured with constant exposure and electronic gain settings at 20× magnification except for (A) which was at 40×.

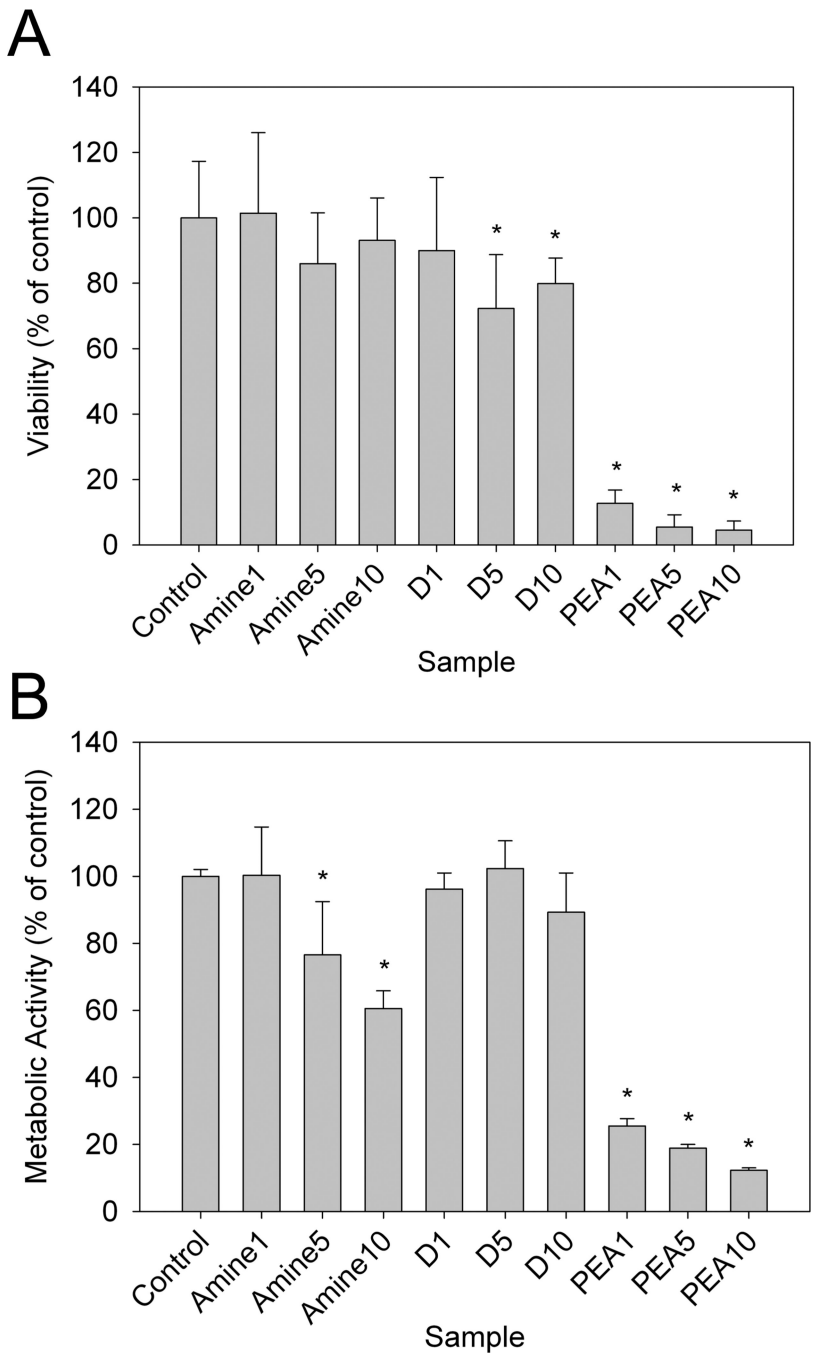

Figure 6.

Quantification of cortical neuron viability after 24 hours of exposure to iron oxide nanoparticles with varying surface chemistry. (A) Viability quantified by the percent area of each image covered by fluorescently labeled cells. (B) Metabolic activity as assessed by changes in the absorance of light by the MTS solution. All PEA samples significantly reduced viability as quantified by either metric. All data represent the mean ± SD normalized to the control. * Indicates $p<0.05$ as compared to the control.

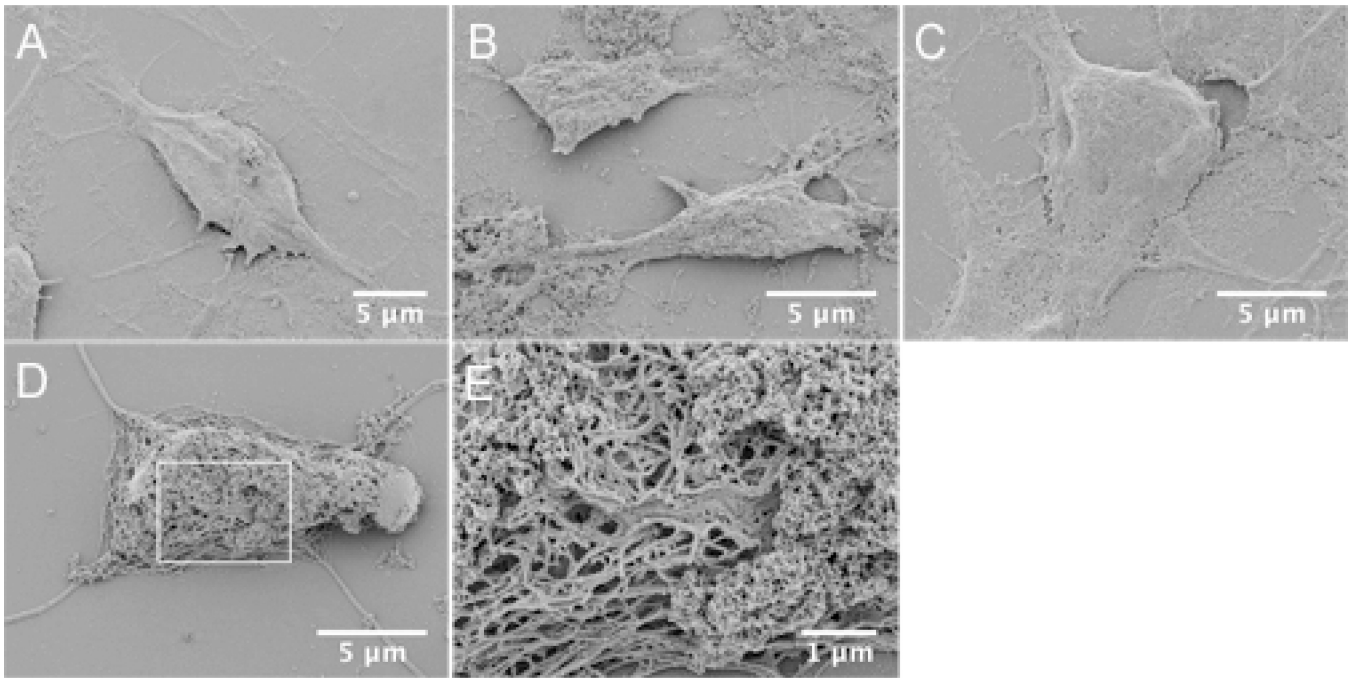

Figure 7.

Scanning electron microscopy (SEM) images of cortical neurons after 24 hours of exposure to iron oxide nanoparticles with varying surface chemistries. Images of (A) control (B) Amine (C) D and (D & E) PEA particles all at 5% (v/v). The outline in (D) represents the area from which (E) was captured. The PEA particles remove the plasma membrane exposing the cytoskeletal network below while all other groups remain intact. Image (A) was captured at 10kX magnification while images (B–D) were captured at 15KX and (D) was at 50kX. Large agglomerates of particles are found on cytoplasm of (D) and in (E).

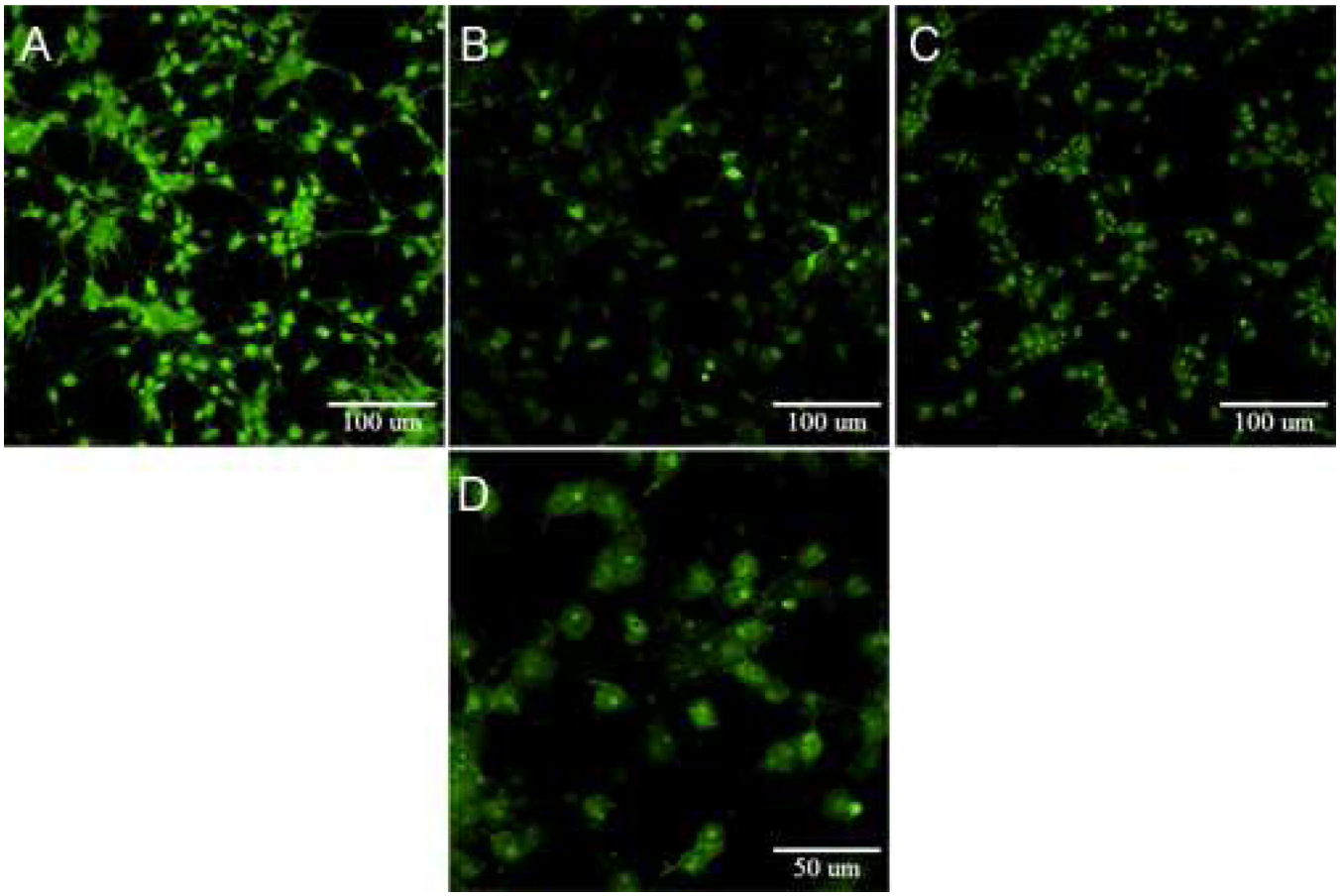

Figure 8.

Assessment of membrane disruption in cortical neurons by the release/retention of fluorescent calcein-AM. Images of (A) control and (B) 5% (v/v) PEA, one hour after administration of particles; (C) and (D) 8 hours after administration of 5% PEA particles. As the membrane is disrupted the brightness of each cell is reduced and after 8 hours the nuclei are clearly visible as bright dots in (D), indicating complete removal of the plasma membrane by the PEA particles. All images were captured with constant exposure and electronic gain settings at 20× magnification except for (D) which was at 40×.